Predictive Modeling of Yoga's Impact on Individuals with Venous Chronic Cerebrospinal System

Sanjun Qiu*
Guangxi Police College, Nanning Guangxi, 530028, China

***Abstract*—People leading a modern lifestyle often experience varicose veins, commonly attributed to factors associated with work and diet, such as prolonged periods of standing or excess weight. These disorders include elevated blood pressure in the lower extremities, especially the legs. An often-researched metric associated with these illnesses is the Vascular Clinical Severity Score (VCSS), which is connected to discomfort and skin discolorations. However, yoga appears to be a viable way to prevent and manage these problems, significantly lessening the negative consequences of varicose veins. The investigation of yoga's effect on VCSS in this study uses a novel strategy combining machine learning with the Extra Tree Classification (ETC), which is improved by the Cheetah Optimizer (CO) and Black Widow Optimizer (BWO). In this study, the ETC model was combined with previously mentioned optimizers, and two models were amalgamated, referred to as ETBW and ETCO. Through the evaluation of the performance of these models, it was discerned that the accuracy measure for prediction was associated with the ETCO model in the context of VCSS. By revealing subtle correlations between yoga treatments and VCSS results, this multidisciplinary approach seeks to provide a thorough knowledge of preventative and control processes. This research advances the understanding of vascular health by correlating yoga interventions with VCSS outcomes using machine learning and optimization algorithms. By enhancing predictive accuracy, it promotes multidisciplinary collaboration, personalized medicine, and innovation in healthcare, promising improved patient care and outcomes in varicose vein management.**

Keywords*—Yoga; varicose veins; Extra Tree Classification; cheetah optimization algorithm; Black Widow Optimizer

I. Introduction

Recently, easy access to food, time constraints, and prolonged working hours have led to individuals' prevalent consumption of fast food and minimal physical exercise [1]. This lifestyle, characterized by improper dietary choices and an absence of physical activity, is identified as the origin of various diseases, including but not limited to diabetes, heart disease, and varicose veins [2].

Varicose veins, influenced significantly by factors such as excessive body weight and prolonged periods of standing or sitting, emerge as one of the most widespread afflictions among individuals [3]. Lifestyles characterized by these factors predominantly cause this condition [4]. Typically manifesting in the lower limbs, particularly the legs, varicose veins exhibit outward characteristics such as skin discoloration and dilated vessels [5]. Subsequently, elucidating the definition reveals that varicose veins are enlarged and twisted veins commonly observed in the legs [6]. Legs are the most frequent location for varicose veins, which are twisted, swollen veins that can cause pain and cosmetic issues [7], [8].

Varicose veins, the signs and symptoms, and possible therapies can be managed and avoided by being aware of this prevalent vascular issue [9]. On the other hand, Chronic venous insufficiency (CVI) [10] describes a condition that affects the venous system of the lower extremities, with the sine qua non-being persistent ambulatory venous hypertension causing various pathologies, including edema, pain, skin changes, and ulcerations [11]. CVI often indicates the more advanced forms of venous disorders, including hyperpigmentation, venous eczema, lip dermatosclerosis, atrophied blanche, and healed or active ulcers [12].

Nevertheless, due to incompetent valves and heightened venous pressure in varicose veins, the term CVI encompasses the complete spectrum of manifestations associated with CVD. Investigating the possible medical advantages connected to yoga practice addresses whether yoga helps treat varicose veins [13]. Yoga stretches are thought to have a moderating effect on the pain and swelling that are frequently linked to varicose veins [14]. The benefits of some yoga poses, especially those involving leg elevation, are highlighted in particular for treating venous issues. Upon examining the physiological elements, it is observed that elevated legs facilitate blood return to the heart, thereby reducing vein pressure and potentially preventing the worsening of varicose veins [15], [16]. Yoga is offered as a supplemental treatment for varicose veins [17], understanding that although it cannot treat the problem, it may significantly lessen its symptoms and possibly even prevent further worsening. It is emphasized that anybody considering adding yoga to their regimen for managing varicose veins should see a healthcare provider or a vain specialist to ensure these poses are acceptable for their particular medical situation [18]. The investigation ends with a call for people to submit their ideas and observations on how well yoga works to treat varicose veins.

The yoga intervention consists of movements designed to target stimulating reflex therapy, reduction of muscular tension, and elasticity in the joints [19]. Exercises for loosening the joints and releasing tense muscles comprise ankle, wrist, elbow, neck, knee, and shoulder motions [20]. Techniques for Shavasana [21] promote profound calmness. Exercises for breathing promote better breathing patterns, tighten the core muscles, and soothe the muscles in the arms and shoulders [22]. Workouts for tightening the powers of the hips, thighs, calves, and abdomen help to reduce stiffness and increase flexibility in action. Numerous asanas (poses) are used to develop multiple muscle groups, extend and rest back muscles, and mobilize cervical

joints [23]. A profound state of sleep is induced, venous return is increased, and prana is balanced in the body through pranayama and other activities. Lastly, for mental relaxation, OM meditation is given [24]. This holistic approach promotes flexibility, relaxation, and general well-being by addressing mental and physical elements.

Machine learning (ML) approaches serve a crucial and pioneering function in addressing the complexities of diverse challenges encountered in real-world problems [25], [26]. In the context of this research, the primary objective was to leverage ML techniques to develop a robust approach capable of predicting and classifying the impact of yoga on the VCSS within a specific group of workers. Recognizing the profound importance of prioritizing workers' health, the study highlights the direct correlation between their well-being and the efficiency and productivity of their work. The choice of the ETC model for this investigation was driven by its practicality in effectively predicting the intricate variability present in the dataset [27]. Two novel optimization algorithms were seamlessly integrated into the ETC framework to enhance the model's precision and accuracy further. In order to ensure the objectivity and reliability of the study, performance metrics were rigorously employed, mitigating potential biases. Through this comprehensive analysis, the study leads to a robust conclusion: yoga can positively impact people's health.

In addition, this study employs a systematic approach to select appropriate techniques for the solution. The study first identifies the problem domain—varicose vein management—and recognizes the need for both medical understanding and computational analysis. Leveraging their expertise in both areas, they choose machine learning, specifically the ETC, to capture complex data interactions. Additionally, they integrate advanced optimization algorithms, such as the Cheetah Optimizer (CO) and Black Widow Optimizer (BWO), to enhance predictive capability. By combining these techniques, they create hybrid models that effectively analyze large datasets encompassing yoga interventions and Vascular Clinical Severity Score measurements. This thoughtful selection process ensures the integration of cutting-edge methodologies tailored to the complexities of the research problem, ultimately leading to a robust and innovative solution.

II. Data Collection and Methodology

A. Data Gathering

When assessing the effects of yoga on people with VCSS, many input parameters were taken into account to identify changes that occurred both before and after the introduction of yoga into their daily habits. Important factors, including weight, height, age, sleep quality, smoking status, VCSS scores before the yoga intervention, food habits, and the number of hours spent sitting and standing throughout the workday, were all included in the inputs. The data from the participants showed a brief picture of their health profile before introducing yoga. Their age, height, weight, and eating habits revealed information on their physical attributes and food preferences. Important lifestyle aspects such as alcohol use and smoking status were taken into account, providing a thorough insight into their behaviours. The quality of sleep was evaluated to evaluate how rest affects general well-being.

Furthermore, the VCSS scores of the individuals before beginning yoga were used as a reference point to assess how beneficial yoga was for venous health. They revealed their daily activity levels by tracking their time standing and sitting throughout work hours. An evaluation was conducted after the subjects started yoga to forecast any prospective changes in them. The impact of yoga on their sleep quality and general lifestyle was considered when forecasting favourable results. The purpose of assessing the effect of yoga on VCSS scores was to assess possible advantages on venous health. Variations in sitting and standing hours following yoga were anticipated to mirror individual activity pattern changes. This predictive study was conducted to provide insight into the possible changes in people's health profiles when they go from not practising yoga to doing it regularly. With an emphasis on venous health, as shown by VCSS scores, the evaluation sought to capture the holistic benefits of yoga on participants' well-being by considering these many input elements. In Fig. 1, a correlation matrix is presented, providing a visual representation for the analysis of relationships between input and output variables.

B. Black Widow Optimization (BWO)

The medium-sized black widow spider, belonging to the Orygiidae family, is prevalent in European countries around the Mediterranean. Female spiders predominantly reside in webs, breeding, feeding, and rearing offspring. The mating process involves web narrowing and potential cannibalism. The Black Widow Optimization method, introduced by Hayyolalam and Kazem in 2020 [28], models spider life cycles for optimization problem-solving, aligning with Darwin's evolutionary theory and demonstrating genetic adaptation in spider populations through competitive growth. The BWO algorithm involves population setup, reproduction, homicide, and mutation stages [29].

1) Initialization: $W_{N\times D} = [X_1, X_2, \dots, X_N]$ has N widows in the number of spiders. $X_1, X_2, \dots, X_N$. D symbolizes an optimization problem's complexity. Within the populace, $X_i = [x_{i,1}, x_{i,2}, \dots, x_{i,D}](1 \le i \le N)$ stands for the widow $i-th$. Every component in a single $[x_{i,1}, x_{i,2}, \dots, x_{i,D}](1 \le i \le N)$ is set up using Eq. (1).

$$x_{i,j} = l_j + rand(0,1) \cdot (u_j - l_j), 1 \le j \le D \quad (1)$$

where, $L = [l_1, l_2, \dots, l_D], U[u_1, u_2, \dots, u_D]$ represent the optimization algorithm's parameters' upper and lower limits.

2) Procreate: Black widows reproduce by a special kind of mating activity. When mating, a pair of spiders designated as the parents of the spiders are chosen randomly from the population to marry by the procreating rate (Pp). Eq. (2) is used to create the progeny.

$$\begin{cases} Y_i = aX_i + (1-a)X_j \\ Y_j = aX_i + (1-a)X_i \end{cases} \quad (2)$$

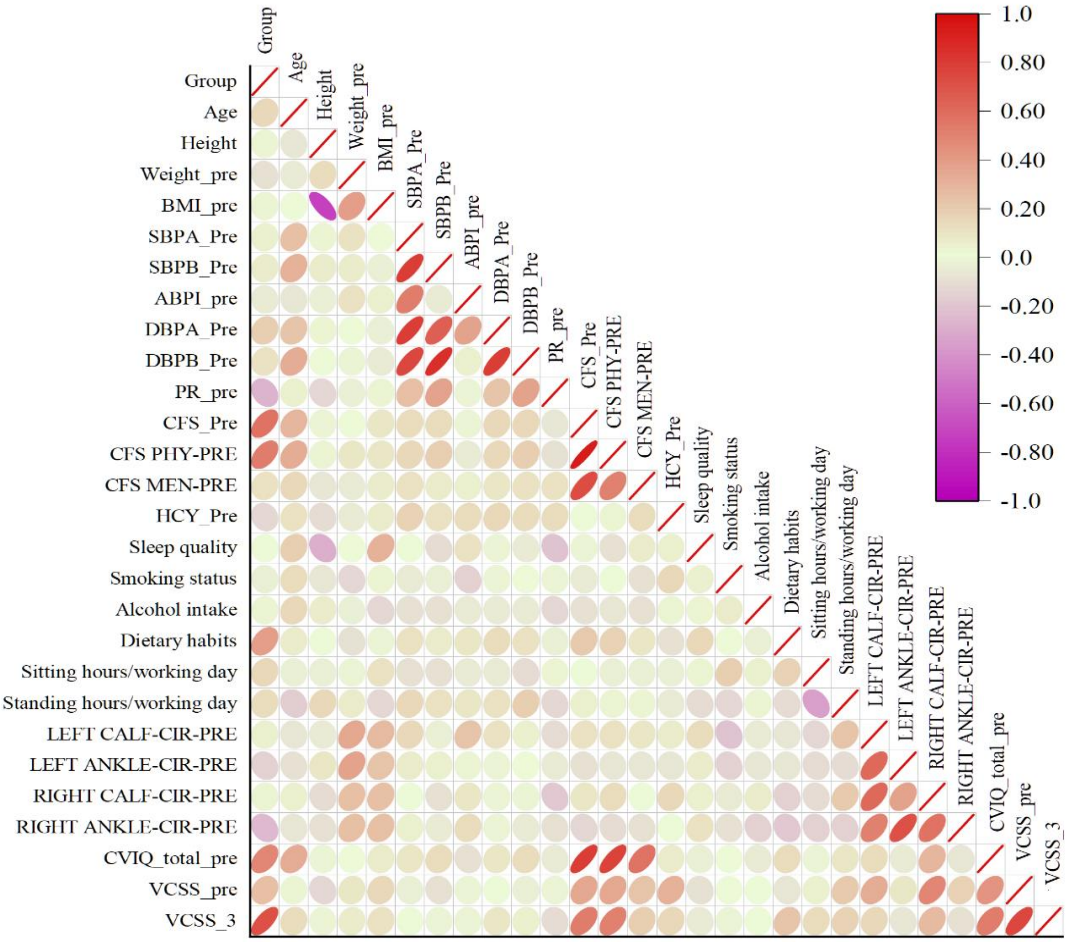

Fig. 1. Correlation matrix to analyze the relationships between input and output variables.

where, spiders X_i and X_j represent the mother and father, respectively. The progeny, through mating, is Y_i and Y_j . Furthermore, α is an array in D dimensions that contains random integers.

3) Cannibalism: Three different types of cannibalism are present at this stage: sibling cannibalism, sexual homicide, and homicide between a mother's kids. The good ones may be kept alive by eliminating the weaker ones.

4) Cannibalization for sex: Following or during mating, the female black widow consumes her spouse. The female spiders that survive are kept for the following generation.

5) Cannibalism of siblings: The more enormous spiders devour their younger ones because of a lack of food supplies or natural adversaries. The strength of a spider is determined by its fitness value. The total number of survivors is calculated using the cannibalism rating (CR) in this procedure.

6) The mother and children engaging in cannibalism: Some young spiders are so powerful that they may even consume their mother. In other words, an answer with a high health value generated by parents will take the place of its mother and be passed on to the following population.

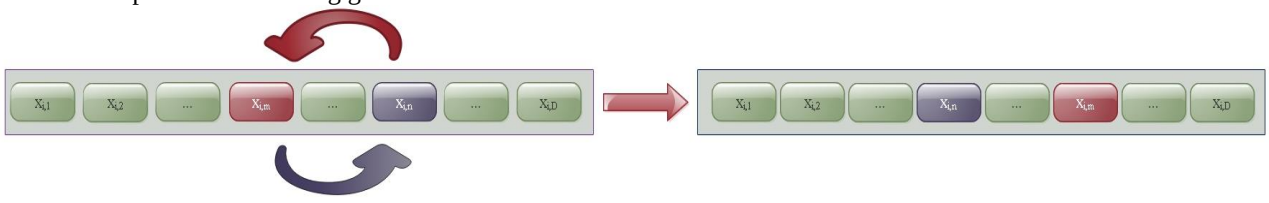

Fig. 2. Mutation method.

7) Mutation: At this point, a constant known as the rate of mutation (Pm) determines how many population members will undergo mutations. Two array elements are chosen randomly and then swapped for the chosen person. The new individuals' fitness is randomly altered, as Fig. 2 illustrates. The BWO algorithm's pseudo-code appears as follows.

Algorithm 1: **The BWO Algorithm**

Input: *Number of populace* (N), *Extreme iteration count* (T), *rate of rate of Mutation* (Pm)
Output: *almost perfect solution for the goal function*

Begin
Initialize the population of black widows at random using Eq. (1);
While $(t < T)$
Determine how many copies there are nr using Pp as a guide;
Pick the population's nr parents;
For $i = 1$ *to nr, do*
From the NR parents, choose two at random to be the parents;
Create kids utilizing Eq. (2);
Destruction of dads;
Eliminate a few of the kids based on CR;
End for
Preserve the surviving women and kids in a fresh matrix as the nex
Determine the quantity of minor nm − based Pm mutations;
For $i = 1$ *to nm*
Choose a response from the kids who are still there;

Create a new solution by randomly changing one of the solution's c
End for
Provide the optimal response;
End while
Provide the optimal response;
End

C. Cheeta Optimization Algorithm (CHO)

1) Overview of the CO Algorithm: The CO method, a potent optimization technique for imitating particular cheetah-hunting strategies, was recently created by Akbari et al. [30]. This algorithm uses three crucial tactics: hunting for prey, waiting, and attacking. Departing the prey and going home is introduced by the algorithm to prevent becoming stranded in local optimum positions. This section first explains the CO algorithm's mathematical model before presenting the ICO algorithm. The answer to the issue is comparable to each cheetah's likely hunting arrangements. It is thought that one's position within the population determines the prey (best answer). During the hunting season, cheetahs modify their potential groupings to maximize efficiency.

2) Searching strategy: A cheetah looks for appropriate prey depending on its hunting style and the state of the environment. The searching stage of a mathematical model corresponds to this:

$$X_{i,j}^{t+1} = X_{i.j}^{t} + \hat{r}_{i,j}^{-1} \cdot \alpha_{i,j}^{t} \quad (3)$$

where, $X_{i.j}^{t}$ denotes the cheetah i at chasing time t and $X_{i,j}^{t+1}$ is the new arrangement. The randomization parameter is the inverse of a regularly distributed random number, $\hat{r}_{i,j}^{-1}$. Other than that, $\alpha_{i,j}^{t}$ defines the random length of the steps and is stated as follows for the leader:

$$\alpha_{i,j}^{t} = 0.001 \times t/T \times \left(U_j - L_j\right) \quad (4)$$

Where the variable $j's$ upper and lower bounds are denoted by U_j and L_j , respectively. T is a representation of a hunting time. The random length of steps for additional cheetahs in a group is determined by calculating the distance between cheetah i and a randomly chosen cheetah k in the group.

$$\alpha_{i,j}^{t} = 0.001 \times t/T \times \left(X_{i,j}^{t} - X_{k,j}^{t}\right) \quad (5)$$

3) Sitting-and-waiting strategy: Cheetahs hunt quickly. It takes much energy to be fast and flexible during the pursuit. As such, the attack and pursuit cannot last for an extended period. Because of this, waiting till the prey is sufficiently close to them is one of the cheetah's essential hunting methods. They then launch the assault. This behaviour can boost the success of hunting and is represented as follows:

$$X_{i,j}^{t+1} = X_{i,j}^{t} \quad (6)$$

4) Attacking strategy: Cheetahs strike their prey at the right moment. When attacking, the cheetah uses two essential characteristics, speed, and flexibility, to its advantage. Since cheetahs need to get as near their prey as possible in the least amount of time, they attack at full speed. Here, the prey becomes aware of the cheetah's onslaught and begins to flee. Since the cheetah is so close to its target and moves quickly, the prey chooses to make a quick turn to escape. As a result, the cheetah places its prey in precarious situations and uses its great degree of flexibility to grab it. Attacks can occur alone or in clusters. In response to the prey's location, the cheetah's position changes in single attack mode. Depending on the prey's and other group members' state, this can be done dynamically in a group assault.

$$X_{i,j}^{t+1} = X_{B,j}^{t} + \check{r}_{i,j} \cdot \beta_{i,j}^{t} \quad (7)$$

$$\check{r}_{i,j} = \left|r_{i,j}\right|^{\exp(\frac{r_{i,j}}{2})} \sin(2\pi r_{i,j}) \quad (8)$$

When the prey location is denoted by $X_{B,j}^{t}$, the turning factor, $\check{r}_{i,j}$, represents the prey's abrupt shifts during its flight, and $r_{i,j}$ is a chosen at random number drawn from a normal distribution. Eq. (20) defines the interaction factor as $\beta_{i,j}^{t}$, which may be represented as follows:

$$\beta_{i,j}^{t} = X_{k,j}^{t} - X_{i,j}^{t} \quad (9)$$

5) Strategy selection mechanism: In the CO algorithm, selecting the best course of action is done at random. Assume two random integers from a uniform distribution, r_2 and r_3. The sit-and-wait approach is used if r_2 is larger than r_3; if not, one of the hunt or assault tactics is implemented. Between the two assault and search tactics, a condition is determined by the H element (see Fig. 3). The following expression describes how this component declines with time:

$$H = e^{2\left(1-\frac{t}{T}\right)}(2r_1 - 1) \quad (10)$$

where, r_1 is a random number between 0 and 1. Between these two approaches, a situation has been established such that, come hunting season, searching is the more likely option. It seems conceivable that an attack will happen as the hunting season continues.

D. Performance Evaluators

Different evaluation criteria are available for evaluating the performance of classifiers. A popular statistic for assessing the

efficacy of a machine learning algorithm is the accuracy indicator, which computes the proportion of adequately predicted observations. Recall, Accuracy, and Precision are often utilized indicators. Accuracy represents the entire correctness of the model. It displays the percentage of correctly predicted instances in each case, including genuine positives and true negatives. Accuracy is an important metric, but imbalanced datasets might render it inadequate.

$$Accuracy = \frac{TP + TN}{TP + TN + FP + FN} \quad (11)$$

Precision is used to measure how effectively the model forecasts positive results. The ratio of accurately anticipated favourable results to all optimistic forecasts is calculated. Less false positives indicate a model with high accuracy.

$$Precision = \frac{TP}{TP + FP} \quad (12)$$

The model's ability to recognize each relevant instance of the category of positives is measured by recall. It computes the ratio of correctly predicted positive observations to all positive ones. A decent measure of how few erroneous outcomes the model produces is recall.

$$Recall = TPR = \frac{TP}{P} = \frac{TP}{TP + FN} \quad (13)$$

The F1-score is the recall and accuracy harmonic average. It provides precision and recall in balance. When there is an uneven distribution of classes, this metric is beneficial since it accounts for erroneous positives and false negatives.

$$F1\ score\ = \frac{2 \times Recall\ \times\ Precision}{Recall + Precision} \quad (14)$$

The letter TP in the previous equations indicates a favourable prognosis that matches the positive result. The acronym FP denotes an optimistic forecast in scenarios with adverse outcomes. A pessimistic prediction with TN indicates one similar to the actual negative outcome. A negative forecast is denoted by the sign FN when the accurate result is positive.

III. Results

A. Models Comparison

As previously mentioned, VCSS is one of the most prevalent conditions among individuals. Various causes, such as an incorrect lifestyle, lack of exercise, and genetic factors, contribute to the development of VCSS. Aggressive treatments, including surgery and laser interventions, are deemed beneficial, although they carry inherent complications. In this context, the recommendation of yoga arises. This exercise is proposed due to its efficacy in alleviating pressure in the lower limbs, particularly the legs, ultimately contributing to the control and enhancement of the patient's condition. The base model, ETC, and two combined models, ETBW and ETCO, are employed to assess the accuracy of predictions. The evaluation focuses on individuals who have not incorporated yoga into their routines. Table I illustrates the model ranking, indicating which model achieves the highest accuracy and optimal performance based on metric values. This analysis provides a comprehensive overview of the predictive capabilities of the models, shedding light on their effectiveness in the absence of yoga intervention. As demonstrated in Table I, the performance of each model is assessed across three severity conditions: absent, mild, and moderate to severe. The ETC model exhibits a precision value of 0.846 in the absent condition, 0.905 in the mild condition, and 0.30 and 1000 precision values in the moderate and severe conditions, respectively.

Conversely, when incorporating BWO into the base model, there is an enhancement in conditions accuracy. Notably, the precision value increases in the absent condition from 0.846 to 0.917. It experiences a marginal change from 0.905 to 0.907 in the mild condition. However, in moderate and severe conditions, the precision value of the ETBW model remains consistent with that of the ETC model, indicating a limited impact of this model on the base model's effectiveness. The recall and F1 score values for both the ETC and ETBW models in the absent and severe conditions are identical, a pattern replicated in the severe condition for the ETCO model concerning precision, recall, and score values.

TABLE I. Evaluation Indexes of the Developed Models' Performance based on Positions VCSS. PRE

Model	Condition	Metric value		
		Precision	***Recall***	***F1-score***
ETC	Absent	0.846	0.917	0.880
	Mild	0.905	0.905	0.905
	Moderate	0.930	0.909	0.920
	Severe	1.000	1.000	1.000
ETBW	Absent	0.917	0.917	0.917
	Mild	0.907	0.929	0.918
	Moderate	0.930	0.909	0.920
	Severe	1.000	1.000	1.000
ETCO	Absent	0.786	0.917	0.846
	Mild	0.929	0.929	0.929
	Moderate	0.976	0.932	0.954
	Severe	1.000	1.000	1.000

Regarding the ETCO model, a discernible retrogression in precision value is evident in the absent condition, attributable to the combination with the COA optimizer, despite the higher accuracy achieved compared to the base model. The precision, recall, and F1-score values remain consistent at 0.929 in mild conditions, showcasing equivalent performance. Notably, the ETCO model excels in moderate conditions, recording the highest values across all three metrics: precision (0.976), recall (0.932), and F1-score (0.954). This pattern implies that the optimizers exhibit limited efficacy in severe conditions, and metric values do not witness a discernible increase. ETCO demonstrates superior performance among the four models, with ETBV showcasing the highest accuracy in the absent condition and ETCO registering a minor favourable performance in this category. It should be noted that these values pertain to individuals who have not initiated yoga practice.

Incidentally, Table II forecasts the anticipated performances of the models following a three-month yoga intervention, revealing distinct outcomes. In the ETC model, precision values experience a notable shift, reaching 0.918 in the absent position, 0.864 in the mild position, and 0.954 and 1.000 in the moderate and severe positions, respectively. Conversely, the ETBW model demonstrates diminished accuracy in the absent positions, registering a precision value of 0.914. However, parity is observed in the moderate position, with a precision value of 0.954, and identical precision values are observed in the severe positions. The precision, recall, and F1-score values for the absent position are maintained at 0.914, reflecting identical metrics achieved by ETBW models in the corresponding positions.

Additionally, in the mild position, superior performance is demonstrated by the ETCO model compared to other models. This superiority is upheld by the model in the F1 score value for the moderate position, and an equal recall value is shared in the same position with the ETBW model. In contrast, lower performance is exhibited by the ETC and ETBW models in the mild position, with a recorded recall value of 0.826. The highest accuracy in recall value is observed in the moderate position of the ETCO model, registering a measured value of 0.988. Hence, it becomes evident that a notable enhancement is exhibited by the ETCO model compared to other models, suggesting that the COA optimizer is more effective in augmenting the base model than the BWO optimizer.

B. Visual Representation of Model's Performance

Fig. 3 displays the performance of developed models across two-time scales: initially, among individuals who had not engaged in yoga, and subsequently, three months after initiating yoga practice. Each model is compared within these two-time scales. For instance, the ETCO model exhibits higher accuracy, recall, and F1 score in the test grade with a value of 0.967. However, the current model does not demonstrate optimal performance after three months. Specifically, the ETCO model performs best in the Train phase for all four metric values in the VSS.3 target.

In the current target, the lowest value pertains to the F1 score in the test phase, with a value of 0.898. Conversely, the lowest values in VCSS.PRE targets are observed in recall and accuracy during both test and train phases, with a value of 0.914. In the VCSS.PRE target, the best performance in the training phase, is demonstrated by the ETBW model, with a precision value of 0.930, followed closely by accuracy, recall, and F1 score, each with a minimal difference at 0.929 in the same phase. In the test phase, all four metrics exhibit nearly identical values. In another target within the same phase, the F1 score registers a lower value of 0.898, while recall and accuracy metrics share a value of 0.9. In the VSS.3 target, the performance of each of the three models closely mirrors one another. The ETC model attains its highest value in precision for both the test and train phases, reaching 0.918 in the VCSS.PRE target.

Conversely, the lowest accuracy is associated with the precision value across all phases, standing at 0.911. Furthermore, the lowest value is in the VCSS.3. Three targets is 0.9, attributed to accuracy and recall in the test phase. Ultimately, the highest accuracy in the second target is linked to recall and accuracy, both attaining a value of 0.929.

TABLE II. EVALUATION INDEXES OF THE DEVELOPED MODELS' PERFORMANCE BASED ON POSITIONS. VCSS.3

Model	**position**	**Metric value**		
		Precision	***Recall***	***F1-score***
ETC	Absent	0.918	0.886	0.899
	Mild	0.864	0.826	0.844
	Moderate	0.954	1.000	0.976
	Severe	1.000	1.000	1.000
ETBW	Absent	0.914	0.914	0.914
	Mild	0.905	0.826	0.864
	Moderate	0.954	1.000	0.976
	Severe	1.000	1.000	1.000
ETCO	Absent	0.914	0.914	0.914
	Mild	0.909	0.870	0.889
	Moderate	0.976	1.000	0.988
	Severe	1.000	1.000	1.000

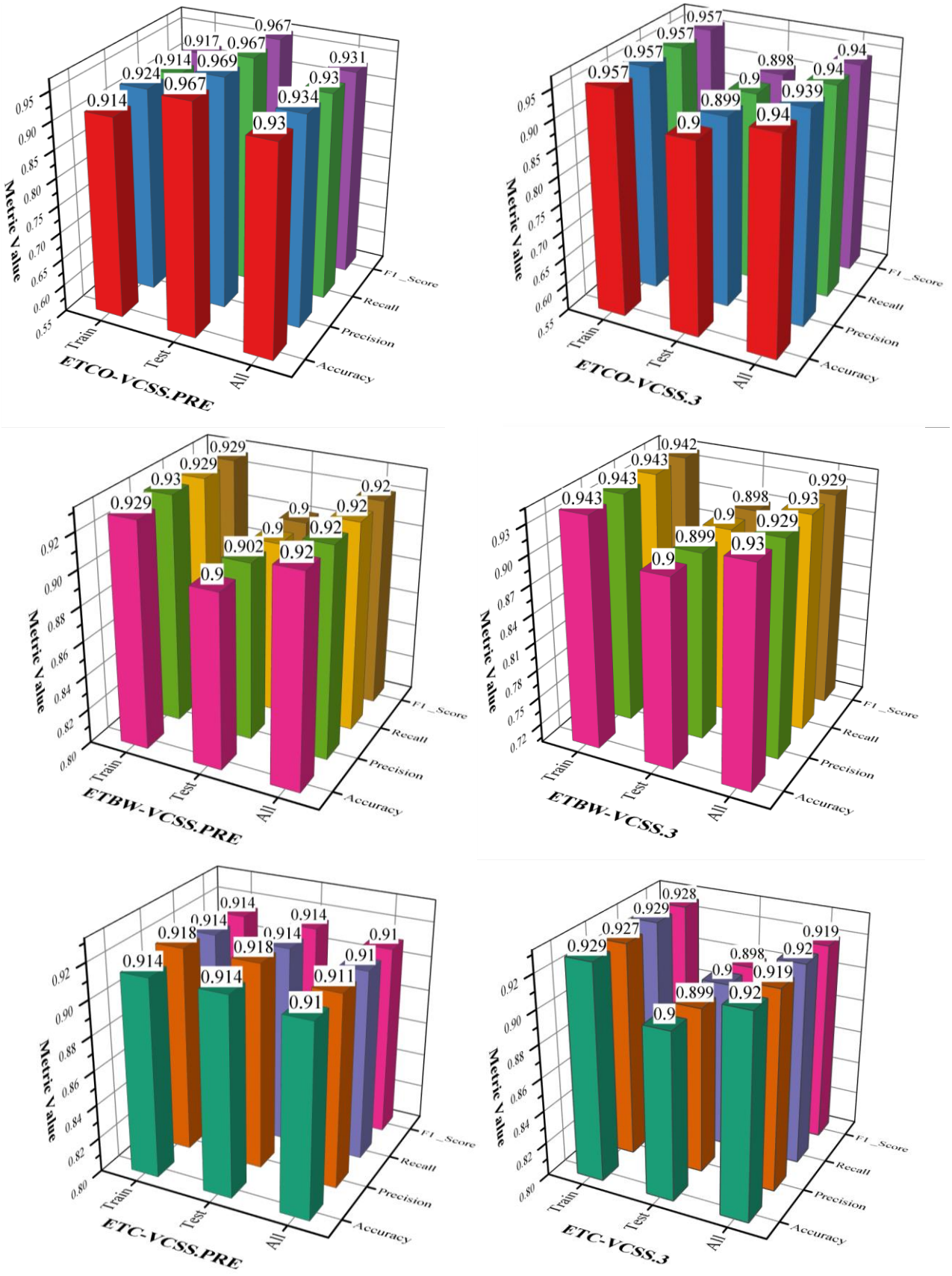

Fig. 3. 3D bar plot to visually assess the performance of the developed models.

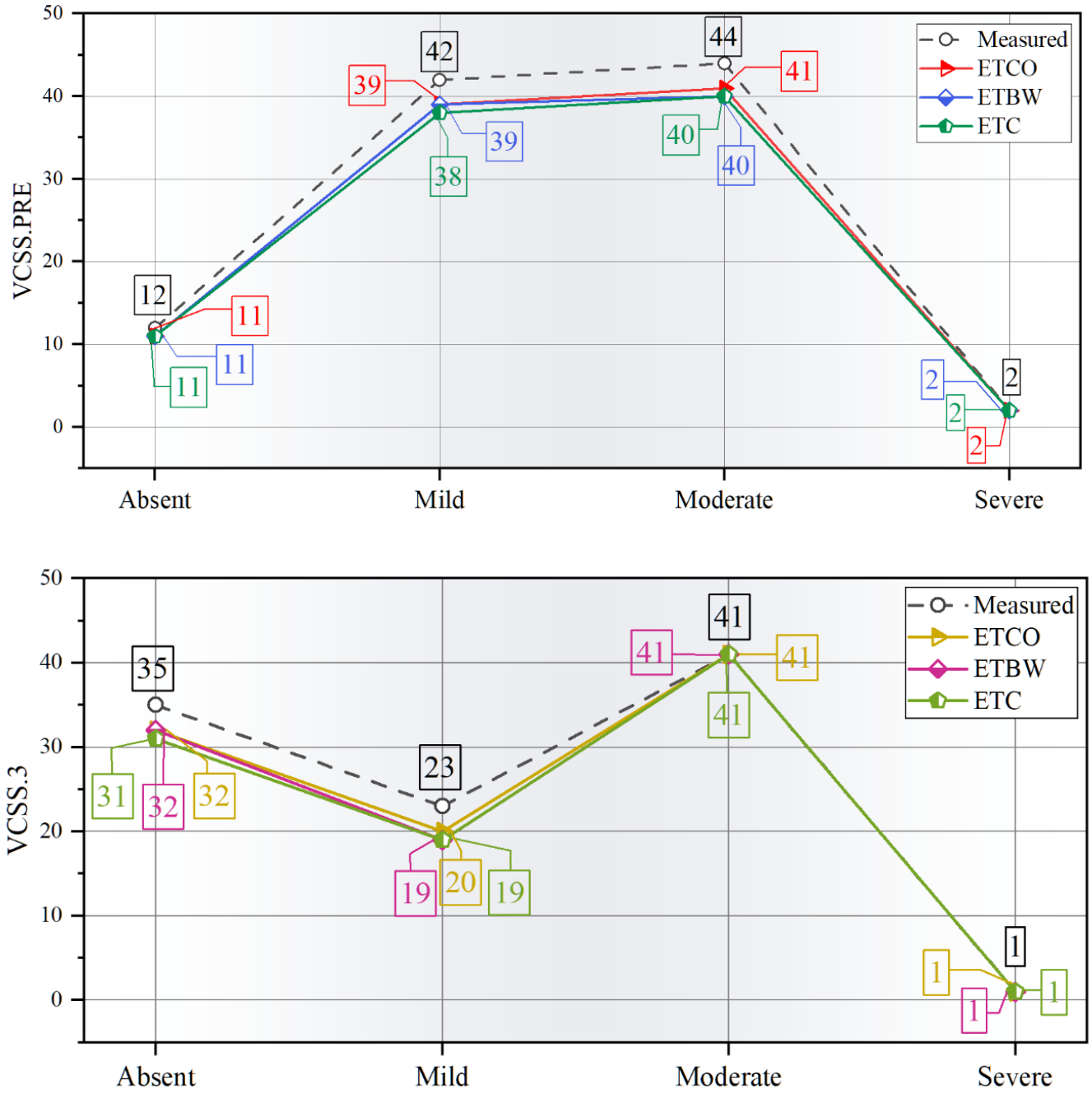

Fig. 4. Line-symbol plot for the correlation of measured and predicted values.

The correlation of measured and predicted values in VCSS.PRE and VCSS.3 targets are depicted in Fig. 4. In this plot, the accuracy of each model is demonstrated across four positions: absent, mild, moderate, and severe, however, in the VCSS.PRE target, the measured accuracy of ETC, ETBW, and ETCO is 11 out of 12, indicating the high prediction accuracy of these three models in the current condition. In the mild condition, 39 out of 42 accuracy is achieved by the ETCO and the ETBW models, signifying high accuracy in the current condition and target. The ETC model holds the second rank, boasting an accuracy of 38 out of 42. Moving to the moderate condition, the highest accuracy is attributed to the ETCO model. In contrast, the ETC and ETBW models exhibit identical accuracy, differing by 2.47% from the ETCO model and 9.52% from the measured accuracy.

Nevertheless, the highest accuracy is attained by each of the three models in the severe condition, achieving a perfect accuracy of 2 out of 2. This signifies that the models demonstrate optimal performance in the severe conditions of the VCSS.PRE target. On the other hand, in the VCSS. For three targets, the optimal performance of each model is evident in both moderate and severe conditions. In the moderate condition, the measured

accuracy is 41 out of 41. In contrast, in the severe condition, the accuracy measured is 1 out of 1. Additionally, in the mild condition, the highest accuracy is achieved by the ETCO model, with a measured accuracy of 20 out of 23. In the absent condition, the best performance is observed in the ETBV and ETCO models, with a measured accuracy of 32 out of 35. Ultimately, upon comparing the models' performance in the VCSS.PRE and VCSS.3 targets, it becomes evident that each of the three models demonstrates its optimal performance in the VCSS.3 target.

For instance, Fig. 5 illustrates the percentage distribution of correctly classified and misclassified values in the VCSS.PRE target, the accuracy of the ETCO model in the absent condition is measured at 91.7%, with 8.3% of participants misclassified. In the mild condition, the accuracy measure is 92.9%, misclassifying 2.3% of participants in the moderate condition and 4.8% in the absent condition. Ultimately, the model's accuracy reaches 100% in severe conditions, indicating that all participants' conditions are correctly predicted. Moving to the ETBW model, it is observed that in the absent condition, the accuracy of the current model is 91.7%, with 8.3% of participants misclassified in mild conditions. 92.9% of participants are correctly predicted in mild conditions, with only 7.1% misclassified in moderate conditions. In moderate conditions, 90.9% of participants are correctly predicted, except for 6.8%, who are misclassified in mild conditions, and 2.3% of participants misclassified in the absent grade.

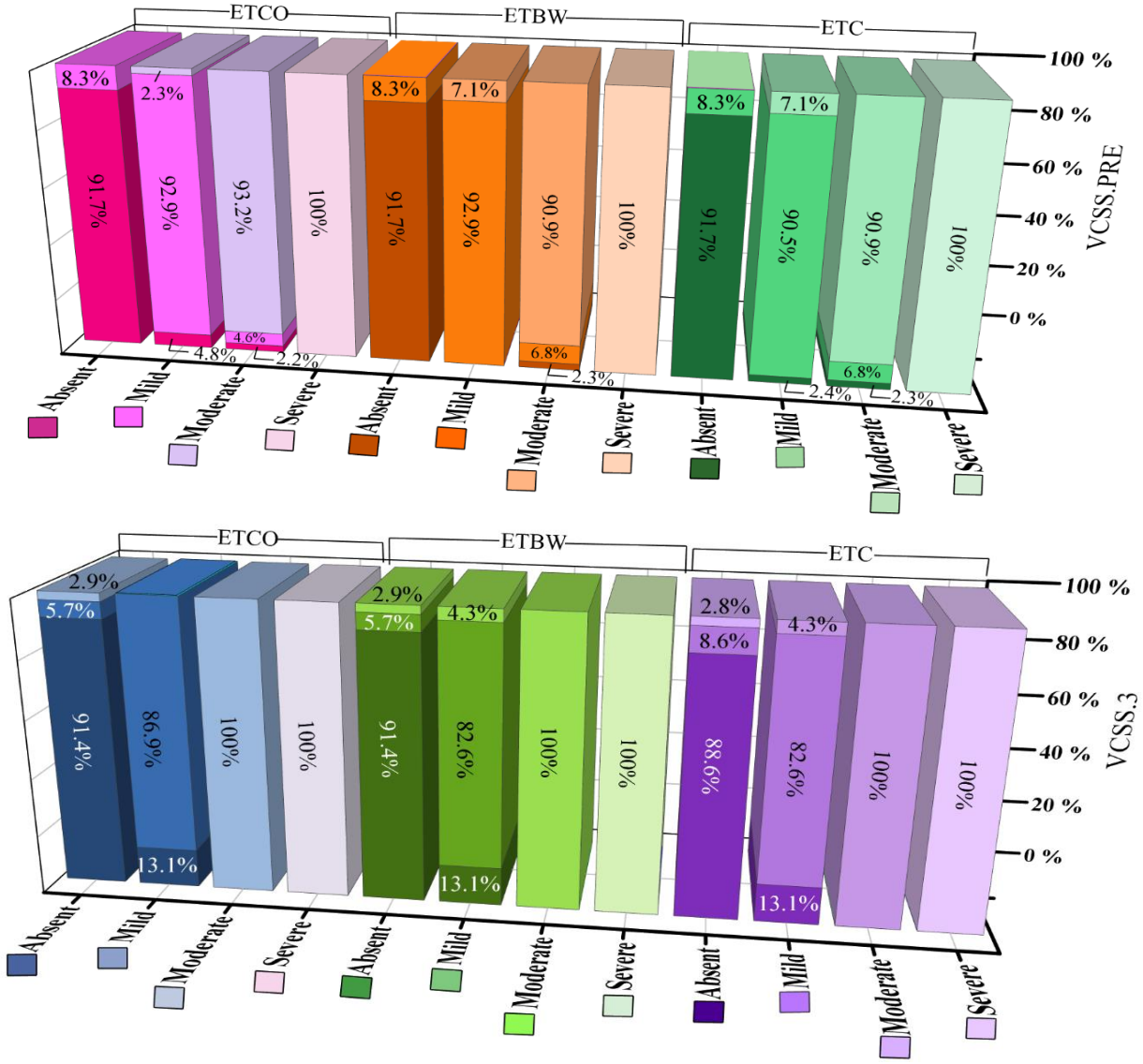

Fig. 5. The 3D stacked bar chart for the percentage distribution of correctly classified and misclassified values.

Nevertheless, in the severe grade, the conditions of all participants are correctly predicted with 100% accuracy. Moving on to the ETC model, similar to other models, participants' conditions in the severe grade are predicted with 100% accuracy. However, 90.9% of participants are correctly predicted in the moderate grade, with 6.8% misclassified in mild conditions and 2.3% misclassified in absent conditions. In mild conditions, 90.5% of participants are correctly predicted, with 7.1% misclassified in the moderate grade and 2.4% misclassified in an absent condition. Ultimately, in the absent

condition, the model demonstrates its highest accuracy, measured at 91.7% after the severe grade, with a misclassification rate of 8.35% for participants in the mild grade.

On the other hand, in the VCSS.3 target, the highest accuracy is observed in severe and moderate conditions for each of the three models, with 100% of participants correctly predicted. The second-highest accuracy is attributed to the ETBW and ETCO models in an absent condition, with 91.4% of participants correctly predicting and misclassifying 5.7% of participants in mild conditions and 2.9% in moderate conditions. However, the lowest accuracy is noted for the ETC and ETBW models in mild conditions, with 82.6% of participants correctly predicting and misclassifying 13.1% of participants in an absent condition and 4.3% in moderate conditions.

The model's categorization threshold is changed to get various pairings of actual positive and false positive rate data. After that, a graph with these pairs drawn displays the ROC curve. When the model performs as well as random chance, the diagonal line shows the situation. A decent classifier should aim for a ROC curve closer to the top-left section, improved accuracy, greater receptivity, and a reduced false positive rate. Computing the area under the ROC curve is customary to offer a single statistic that encapsulates the classifier's overall performance. Fig. 6 represents the ROC curve of the hybrid models.

ROC score closer to 1 indicates that the model can discriminate better in the VCSS.PRE target of the ETCO model, the highest accuracy is associated with the absent condition, achieving a true positive grade of 1.0 at a false positive rate of 0.1. Subsequently, the mild condition attains a true positive rate of 1.0 after a false positive rate of 0.4. At the same time, the lowest accuracy is observed in the moderate condition, reaching a true positive rate of 1.0 at a false positive rate of 0.7.

On the other hand, in the VCSS.3 target, the ETCO model achieves a true positive rate of 1.0 in the moderate condition, within a stable range before a false positive rate of 0.1. The second-highest grade is associated with the absent condition, attaining a true positive rate of 1.0 after a false positive rate of 0.2. At the same time, the lowest accuracy is observed in the mild condition, reaching a true positive rate of 1.0 after a false positive rate of 0.8. Thus, it can be understood that in the VCSS.3 target, the moderate condition exhibits the highest accuracy among the other conditions or classes.

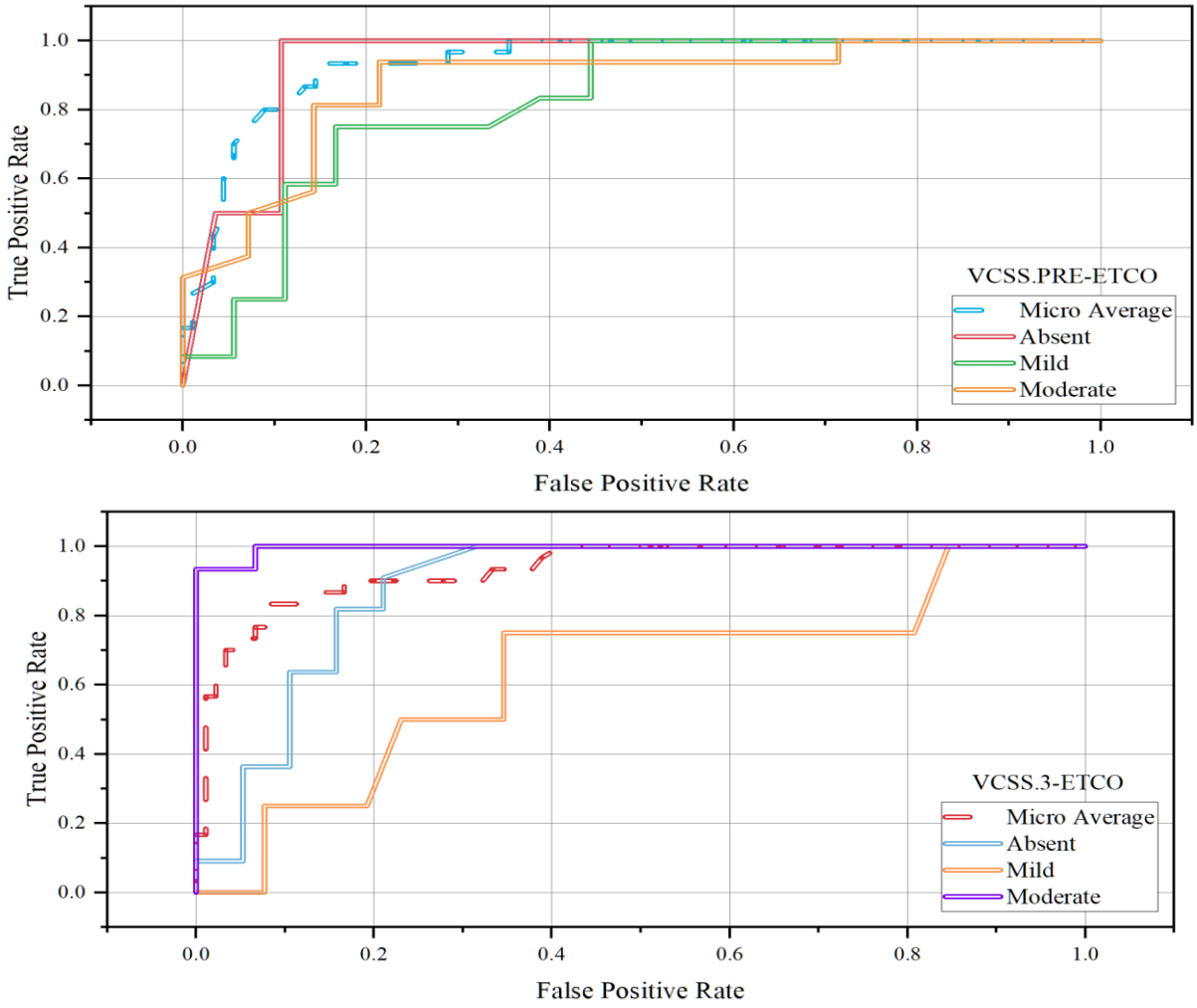

Fig. 6. ROC curve of the best hybrid models.

C. Convergence Curve

Generally speaking, a convergence curve is a graphical depiction of an iterative process's convergence over time. This idea is frequently discussed concerning optimization methods, especially in numerical analysis and machine learning. In the context of optimization algorithms, such as gradient descent, the convergence curve shows how the value of the objective function or the error changes as the algorithm iteratively refines its solution. The x-axis represents the number of iterations, and the y-axis represents the value of the objective function. The curve provides insights into how quickly the algorithm converges towards the optimal solution. The convergence curve in machine learning may be used to track the algorithm's effectiveness while training a model. The curve should, in theory, have a declining trend, signifying that the algorithm is gradually lowering the error or enhancing the data fit. A well-behaved convergence is frequently indicated by a sharp initial drop followed by a steadier decline. Practitioners can benefit significantly from using the convergence curve to evaluate an optimization algorithm's efficacy and efficiency and make well-informed judgments about hyperparameters, halting criteria, and overall model performance.

This section employs the convergence curve to ascertain the correct training of models in various targets. For instance, in Fig. 7, the performance of the combined ETCO and ETBW models in the VCSS.PRE target is illustrated, revealing that the ETCO model achieves a measured accuracy of 0.93 in the 110th iteration. In comparison, the ETBW model reaches an accuracy of 0.8 in the 100th iteration. Consequently, the performance of the ETCO model in the VCSS.PRE target is marginally superior to that of the other model.

Similarly, in the VCSS.3 target, the ETCO model attains a 0.93 accuracy in the 110th iteration, while the ETBW model achieves a measured accuracy of 0.8 in the 111th iteration. This indicates that the ETCO model exhibits higher accuracy in both targets, albeit with a minimal difference between them.

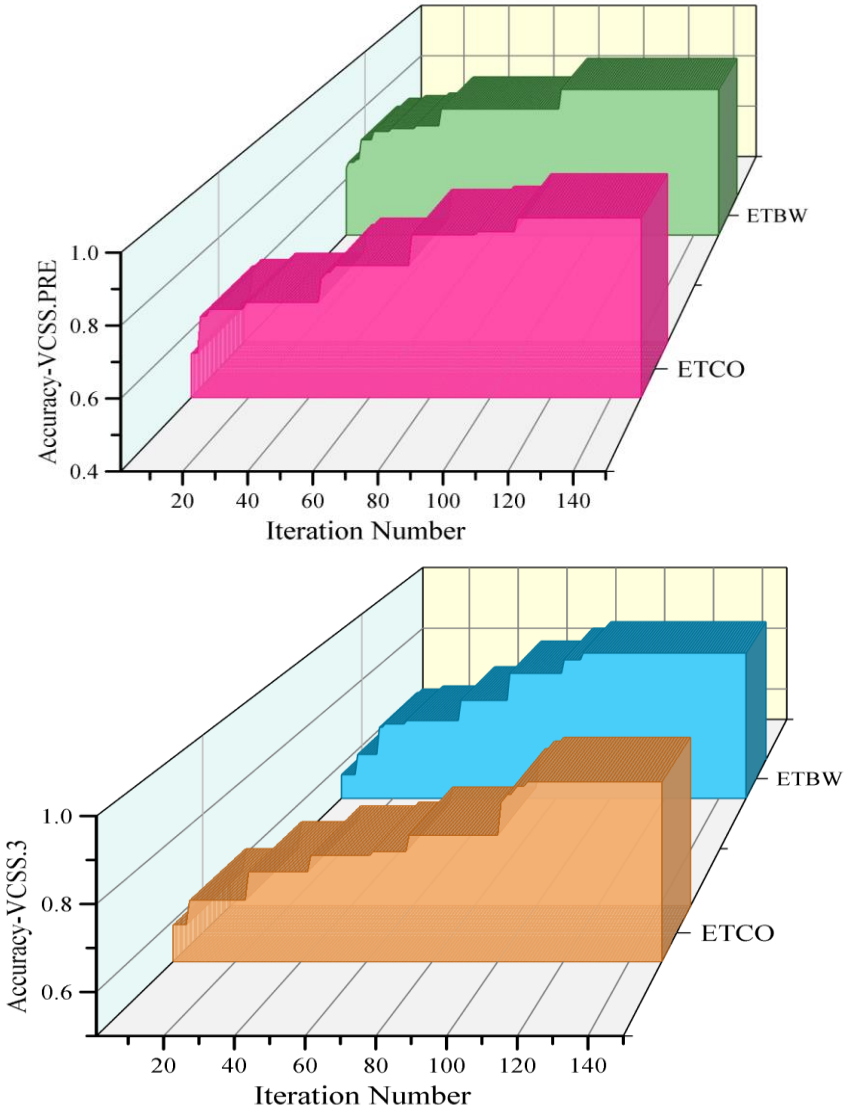

Fig. 7. Convergence curve of hybrid models.

IV. DISCUSSION

A. Limitations

- Generalizability: The study's findings may have limited generalizability due to factors such as sample size, demographics, and specific yoga interventions examined. Further research involving larger and more diverse populations is needed to validate the results across different settings and populations.
- Ethical Considerations: The study raises ethical considerations regarding patient privacy and consent, especially when dealing with sensitive medical data. Researchers must ensure compliance with ethical guidelines and regulations to protect patient confidentiality and rights.
- Interpretation of Results: While the study identifies correlations between yoga interventions and Vascular Clinical Severity Score outcomes, causality cannot be definitively established. Additional research, including randomized controlled trials, is necessary to determine the causal relationship between yoga and varicose vein management outcomes.

B. Application of Study

- Improved Varicose Vein Management: The study's findings offer practical applications for managing varicose veins by highlighting the potential benefits of yoga interventions. Healthcare professionals can use this knowledge to recommend yoga as a complementary approach to traditional treatments, potentially enhancing patient outcomes and quality of life.
- Enhanced Predictive Modeling in Healthcare: The integration of machine learning and optimization algorithms demonstrates the feasibility of using advanced computational techniques to analyze medical data. This approach can be extended to other areas of healthcare, facilitating more accurate predictive modeling and personalized treatment recommendations.
- Multidisciplinary Collaboration: The study encourages collaboration between medical professionals, data scientists, and engineers. This multidisciplinary approach fosters innovation and knowledge exchange, leading to the development of holistic solutions to complex healthcare challenges.

V. CONCLUSION

The utilization of machine learning approaches has yielded important insights into the predictive study of the impact of yoga on the Venous Clinical Severity Score (VCSS). The application of ML algorithms, including the Extra Tree Classification (ETC) model, Black Widow Optimization (BWO), and Cheetah Optimizer Algorithm (COA), has made it possible to comprehend yoga's possible effects on vein health in more detail. Through performance criteria, including recall, precision, and F1 score, the generated models have thoroughly assessed the predicted accuracy under various scenarios. The assessment of the stability and effectiveness of the model is further enhanced by using convergence curves and comparison analysis.

While various optimization strategies may affect the performance of base models under particular circumstances, the overall predictive power of the machine learning models suggests that they may be able to capture the dynamic link between VCSS and yoga involvement. Visually displayed, the performance of the models is assessed, and the ETCO model emerges as the superior performer when compared to other models under identical conditions for the VCSS.3 target. It achieves a training phase accuracy of 0.957. The second position is occupied by the ALL term, attaining values of 0.94 in accuracy, 0.939 in precision, 0.94 in recall, and 0.94 in F1 score. The test grade holds the third position.

Further investigation is advised to determine the long-term effects of yoga on VCSS through more extensive longitudinal studies; to improve external validity, a variety of participant groups should be investigated; comprehensive lifestyle assessments should be included; standardizing yoga protocols will ensure repeatability of results; and cooperation with medical professionals is encouraged for a comprehensive approach. As more research on the benefits of yoga for vein health is conducted, the body of information regarding non-traditional treatments for vein problems expands. This study sets the groundwork for further investigations. Using machine learning to predict yoga's impact on VCSS presents a viable path for preventative and customized healthcare approaches.

In conclusion, the utility of this prediction extends beyond the academic realm, having potential applications in the real-world context. It is believed that specialists and health departments can effectively implement the prevention and control of VCSS through yoga. This proactive approach can potentially mitigate the need for aggressive treatments in patients, thereby emphasizing the predictive model's practical implications and societal benefits.

ACKNOWLEDGEMENT

Presided over the research project of Guangxi Vocational Education Teaching Reform, "Research on the Development and Application of Guangxi Public Security Education Micro-Curriculum", project No. GXGZJG2016B188.

REFERENCES

[1] V. D. Goyal, G. Misra, and A. Pahade, “Vein of Giacomini can lead to the recurrence of varicosities after endovenous laser ablation of varicose veins,” Indian J Thorac Cardiovasc Surg, vol. 39, no. 3, pp. 286–288, 2023.

[2] K. Rithika, S. Saranya, K. Chandramouli, and A. Prasath, “Pressure optimization system for Varicose Veins management,” in 2023 IEEE Region 10 Symposium (TENSYMP), IEEE, 2023, pp. 1–5.

[3] V. S. Sassaki and E. Fukaya, “Varicose Veins: Approach, Assessment, and Management to the Patient with Chronic Venous Disease,” Medical Clinics, vol. 107, no. 5, pp. 895–909, 2023.

[4] E. U. Yusufjanovich and Z. A. Rafiqovich, “The Use of Endovascular Laser Coagulation in the Recurrence of Varicose Veins of the Lower Extremities,” International Journal of Scientific Trends, vol. 2, no. 2, pp. 24–31, 2023.

[5] A. Hammoud, A. Tikhomirov, A. Briko, A. Volkov, A. Karapetyan, and S. Shchukin, “Evaluation of the information content for determining the vascular tone type of the lower extremities in varicose veins: a case study,” Biosensors (Basel), vol. 13, no. 1, p. 96, 2023.

[6] P. Helkkula et al., “Genome-wide association study of varicose veins identifies a protective missense variant in GJD3 enriched in the Finnish population,” Commun Biol, vol. 6, no. 1, p. 71, 2023.

[7] J. Charles et al., "Portal Vein Embolization: Rationale, Techniques, and Outcomes to Maximize Remnant Liver Hypertrophy with a Focus on Contemporary Strategies," Life, vol. 13, no. 2, p. 279, 2023.

[8] M. A. Passman et al., "Validation of venous clinical severity score (VCSS) with other venous severity assessment tools from the American venous forum, national venous screening program," J Vasc Surg, vol. 54, no. 6, pp. 2S-9S, 2011.

[9] P. K. Chatzigakis, A. K. Zianika, G. Geropapas, A. Kalamaras, V. Katsikas, and G. C. Kopadis, "Outpatient treatment of truncal veins insufficiency," Hellenic Journal of Vascular and Endovascular Surgery| Volume, vol. 5, no. 2–2023, p. 45.

[10] M.-L. Kuet, T. R. A. Lane, M. A. Anwar, and A. H. Davies, "Comparison of disease-specific quality of life tools in patients with chronic venous disease," Phlebology, vol. 29, no. 10, pp. 648–653, 2014.

[11] N. M. Bouayed, "How to Treat Pulsatile Varicose Veins of the Lower Limbs," J Vasc Surg, vol. 77, no. 4, pp. 42S-43S, 2023.

[12] R. M. Kaplan, M. H. Criqui, J. O. Denenberg, J. Bergan, and A. Fronek, "Quality of life in patients with chronic venous disease: San Diego population study," J Vasc Surg, vol. 37, no. 5, pp. 1047–1053, 2003.

[13] H. Cramer et al., "Characteristics of women who practice yoga in different locations during pregnancy," BMJ Open, vol. 5, no. 8, p. e008641, 2015.

[14] U. Yamuna, K. Madle, V. Majumdar, and A. A. Saoji, "Designing and validation of Yoga module for workers with prolonged standing," J Ayurveda Integr Med, vol. 14, no. 5, p. 100788, 2023.

[15] J. D. Raffetto and R. A. Khalil, "Mechanisms of lower extremity vein dysfunction in chronic venous disease and implications in management of varicose veins," Vessel Plus, vol. 5, 2021.

[16] M. Ni, K. Mooney, K. Harriell, A. Balachandran, and J. Signorile, "Core muscle function during specific yoga poses," Complement Ther Med, vol. 22, no. 2, pp. 235–243, 2014.

[17] S. Naraga, "International Journal of Current Advance," 2019.

[18] R. Hooda and M. Tripathi, "Role of homeopathy medical system in remedy of varicose vein ulcer," International Journal of Homoeopathic Sciences, vol. 2, no. 1, pp. 29–31, 2018.

[19] H. Wang, "Neural network-oriented big data model for yoga movement recognition," Comput Intell Neurosci, vol. 2021, pp. 1–10, 2021.

[20] S. Newcombe, "The development of modern yoga: A survey of the field," Religion Compass, vol. 3, no. 6, pp. 986–1002, 2009.

[21] G. K. Pal, V. Ganesh, S. Karthik, N. Nanda, and P. Pal, "The effects of short-term relaxation therapy on indices of heart rate variability and blood pressure in young adults," American Journal of Health Promotion, vol. 29, no. 1, pp. 23–28, 2014.

[22] T. Biswas, D. Singh, and M. Jha, "Health Promotion through Yoga," Mind and Society, vol. 3, no. 01–02, pp. 20–22, 2014.

[23] I. Hagen, S. Skjelstad, and U. S. Nayar, "Promoting mental health and wellbeing in schools: the impact of yoga on young people's relaxation and stress levels," Front Psychol, vol. 14, p. 1083028, 2023.

[24] N. Gupta, S. Khera, R. P. Vempati, R. Sharma, and R. L. Bijlani, "Effect of yoga based lifestyle intervention on state and trait anxiety," Indian J Physiol Pharmacol, vol. 50, no. 1, p. 41, 2006.

[25] I. El Naqa and M. J. Murphy, What is machine learning? Springer, 2015.

[26] D. Michie, D. J. Spiegelhalter, and C. C. Taylor, "Machine learning, neural and statistical classification," 1994.

[27] D. Baby, S. J. Devaraj, and J. Hemanth, "Leukocyte classification based on feature selection using extra trees classifier: Atransfer learning approach," Turkish Journal of Electrical Engineering and Computer Sciences, vol. 29, no. 8, pp. 2742–2757, 2021.

[28] V. Hayyolalam and A. A. P. Kazem, "A systematic literature review on QoS-aware service composition and selection in cloud environment," Journal of Network and Computer Applications, vol. 110, pp. 52–74, 2018.

[29] M. Madhiarasan, D. T. Cotfas, and P. A. Cotfas, "Black Widow Optimization Algorithm Used to Extract the Parameters of Photovoltaic Cells and Panels," Mathematics, vol. 11, no. 4, p. 967, 2023.

[30] Z. A. Memon, M. A. Akbari, and M. Zare, "An Improved Cheetah Optimizer for Accurate and Reliable Estimation of Unknown Parameters in Photovoltaic Cell and Module Models," Applied Sciences, vol. 13, no. 18, p. 9997, 2023.